Journal of Cellular Biochemistry 100:1056–1069 (2007)

Apoptotic Signaling in Methylglyoxal-Treated Human Osteoblasts Involves Oxidative Stress, c-Jun N-Terminal Kinase, Caspase-3, and p21-Activated Kinase 2

Wen-Hsiung Chan,* Hsin-Jung Wu, and Nion-Heng Shiao

Department of Bioscience Technology and Center for Nanotechnology, Chung Yuan Christian University, Chung Li, Taiwan

Abstract Methylglyoxal (MG) is a reactive dicarbonyl compound endogenously produced mainly from glycolytic intermediates. MG is cytotoxic through induction of cell death, and elevated MG levels in diabetes patients are believed to contribute to diabetic complications. In this report, we show for the first time that MG treatment triggers apoptosis in human osteoblasts. We further show that MG-induced apoptosis of osteoblasts involves specific apoptotic biochemical changes, including oxidative stress, c-Jun N-terminal kinase (JNK) activation, mitochondrial membrane potential changes, cytochrome C release, increased Bax/Bcl-2 protein ratios, and activation of caspases (caspase-9, caspase-3) and p21-activated protein kinase 2 (PAK2). Treatment of osteoblasts with SP600125, a JNK-specific inhibitor, led to a reduction in MG-induced apoptosis and decreased activation of caspase-3 and PAK2, indicating that JNK activity is upstream of these events. Experiments using anti-sense oligonucleotides against PAK2 further showed that PAK2 activation is required for MG-induced apoptosis in osteoblasts. Interestingly, we also found that MG treatment triggered nuclear translocation of NF-κB, although the precise regulatory role of NF-κB activation in MG-induced apoptosis remains unclear. Lastly, we examined the effect of MG on osteoblasts in vivo, and found that exposure of rats to dietary water containing 100–200 μM MG caused bone mineral density (BMD) loss. Collectively, these results reveal for the first time that MG treatment triggers apoptosis in osteoblasts via specific apoptotic signaling, and causes BMD loss in vivo. J. Cell. Biochem. 100: 1056–1069, 2006.

Key words: methylglyoxal; apoptosis; ROS; JNK; PAK2

Methylglyoxal (MG), a reactive dicarbonyl compound found at high levels in the blood of diabetics, is a metabolic by-product of glycolysis and is also formed in various foodstuffs during processing. Excess MG may present serious toxicological effects, as it depletes glutathione (GSH) via covalent bonding between MG and GSH. MG is more reactive than its parent sugar, showing a stronger ability to cross-link with protein amino groups to form stable end products called advanced glycation end products (AGEs) [Brownlee et al., 1988; Bourajjaj et al., 2003]. Under hyperglycemic conditions, a symptom of diabetes, the levels of cytotoxic aldehydes (such as MG) increase. Because diabetic complications develop at a slow rate, researchers have been able to study the long-term effect of MG on the formation of AGEs [Shipanova et al., 1997; Uchida et al., 1997]. In particular, it appears as though MG-altered proteins are associated with the formation of reactive oxygen species (ROS). Recent data suggest that diabetes may cause impairment of cognitive processes via a mechanism that involves both oxidative stress and AGE formation [Messier and Gagnon, 1996; Gerozissis, 2003]. Thus, high MG levels and subsequent MG-induced cytotoxicity may be at least partially responsible for diabetes-related

Abbreviations used: MG, methylglyoxal; ROS, reactive oxygen species; DCF-DA, 2′,7′-dichlorofluorescin diacetate; JNK, c-Jun N-terminal kinase; PAK, p21-activated kinase; LDH, lactate dehydrogenase; NF-κB, nuclear factor κB; BMD, bone mineral density.

Grant sponsor: National Science Council of Taiwan, ROC; Grant numbers: NSC94-2320-B-033-003, NSC94-2745-M-033-002-URD.

*Correspondence to: Dr. Wen-Hsiung Chan, Department of Bioscience Technology, Chung Yuan Christian University, Chung Li, Taiwan 32023. E-mail: whchan@cycu.edu.tw

Received 5 June 2006; Accepted 19 July 2006

DOI 10.1002/jcb.21114

impairments of cognitive function. In addition, MG toxicity may be involved in diabetes-associated bone loss. Studies investigating the effects of diabetes on osteoporosis have shown that type 1 diabetes patients have high rates of bone resorption and turnover, and decreased bone mineral density (BMD) [Bouillon, 1991; Kayath et al., 1998; Nicodemus and Folsom, 2001]. In addition, a recent report showed that AGEs and their receptor interactions-induced human mesenchymal stem cell apoptosis and subsequently prevented cognate differentiation into many tissue cells including bone [Yamagishi et al., 2005]. However, the effects of MG/glycation on osteoporosis are not yet fully understood, and will require further investigation.

The cytotoxicity of MG is due to its ability to trigger apoptosis [Kang et al., 1996; Okado et al., 1996], apparently via oxidative signaling, as indicated by studies showing that MG-induced generation of ROS triggered apoptosis of embryonic stem cells [Hsuuw et al., 2005], while addition of antioxidants blocked H_2O_2-induced apoptosis [Buttke and Sandstrom, 1994]. Although the precise molecular mechanisms underlying apoptosis have not been clearly defined, a number of cysteine proteases called caspases are thought to play important roles [Martins et al., 1997; Nicholson and Thornberry, 1997], as do members of the Bcl-2 family [Tsujimoto and Shimizu, 2000], which regulate mitochondrial membrane potential changes and the release of mitochondrial cytochrome C by modulating the permeability of the outer mitochondrial membrane. In addition, changes in protein kinase activity can be observed during apoptosis in a variety of cell types [Anderson, 1997], indicating that protein phosphorylation is involved in regulating apoptosis. In particular, the c-Jun N-terminal kinase (JNK) acts as a key component in regulating entry into apoptosis in several cell types [Xia et al., 1995; Verheij et al., 1996; Seimiya et al., 1997]. In addition to JNK, p21-activated kinase (PAK) is activated during apoptosis and may also be involved in apoptotic signaling events [Lee et al., 1997; Rudel and Bokoch, 1997; Tang et al., 1998; Chan et al., 1999, 2000]. Although the direct downstream substrates of the PAKs are largely unknown, recent studies have indicated that PAKs may act as upstream regulators of the JNK and p38 MAPK pathways [Zhang et al., 1995; Frost et al., 1996]. Furthermore, we previously showed that activation of PAK2 is required for the photodynamic treatment (PDT)-induced apoptosis of A431 cells [Chan et al., 2000]. However, although many reports have demonstrated that PAK2 plays an important role in apoptotic signaling, its direct downstream substrates and precise regulatory mechanisms have not yet been elucidated.

In an effort to examine possible connections between high MG levels and loss of bone density in diabetics, we examined the apoptotic effects of MG on human osteoblasts. Our results revealed for the first time that MG treatment triggers apoptotic biochemical changes such as oxidative stress, JNK activation, caspase-9 activation, increased Bax/Bcl-2 protein ratios, mitochondrial membrane potential changes, cytochrome C release, caspase-3 activation, and PAK2 activation in human osteoblasts. Furthermore, in vivo experiments showed that MG treatment could cause BMD loss in an animal assay model, likely via MG-induced cytotoxicity.

EXPERIMENTAL PROCEDURES

Materials

[γ-^{32}P]ATP was purchased from Amersham (Little Chalfont, Buckinghamshire, UK). Dulbecco's modified Eagle's medium (DMEM) and 2′,7′-dichlorofluorescin diacetate (DCF-DA) were obtained from Sigma (St. Louis, MO). The anti-JNK1 (C17) and anti-p-JNK (G-7) antibodies, as well as the alkaline phosphatase-conjugated goat anti-rabbit and anti-mouse immunoglobulin G (IgG) antibodies were purchased from Santa Cruz Biotechnology (Santa Cruz, CA). The anti-PARP antibody was from Cell Signaling Technology (Beverly, MA). The monoclonal anti-cytochrome C antibody (6H2.B4) was from Imgenex (San Diego, CA). Z-DEVD-AFC and SP600125 were obtained from Calbiochem (La Jolla, CA). CDP-Star™ (a chemiluminescent substrate for alkaline phosphatase) was purchased from Boehringer Mannheim (Mannheim, Germany) and bicinchoninic acid (BCA) protein assay reagent was from Pierce (Rockford, IL). Protein A-Sepharose CL-4B was obtained from Pharmacia (Uppsala, Sweden).

Production of Non-Commercial Antibodies

The anti-PAK2 (C15) antibody was produced in rabbits using a peptide (TPLIMAAKEAMKSNR;

synthesized by Genosys Biotechnologies) corresponding to the C-terminal region from residues 510–524 of the human and rabbit PAK2 sequences [Martin et al., 1995; Jakobi et al., 1996]. The anti-PAK2 (N17) antibody was produced in rabbits using a peptide corresponding to the N-terminal region from amino acids 1 to 17 of the human and rabbit PAK2 sequences [Martin et al., 1995; Jakobi et al., 1996]. This peptide (MSDNGELEDKP-PAPPVR) was synthesized using an automated peptide synthesizer (430A; Applied Biosystems) and purified on a preparative C-18 reverse phase high performance liquid chromatography column. A cysteine residue was added to the N-terminus to facilitate coupling of the peptide to keyhole limpet haemocyanin, which was performed as previously described [Reichlin, 1980], using glutaraldehyde as the cross-linker. The anti-peptide antibody was produced and affinity purified as previously described [Yu and Yang, 1994].

Cell Culture and MG Treatment

Human osteoblast cells were cultured at 34°C in a humid 95% air/5% CO_2 atmosphere, in DMEM/F12 medium supplemented with 10% heat-inactivated fetal bovine serum, 2 mM L-glutamine, and 0.3 mg/L G418. For MG treatment, cells ($\sim 5–6 \times 10^6$) were plated on 60 mm culture dishes and incubated in medium containing various concentrations of MG for 24 h. The cells were then washed twice with ice-cold PBS and lysed in 600 μl of lysis solution (20 mM Tris-HCl, pH 7.4, 1 mM EDTA, 1 mM EGTA, 1% Triton X-100, 1 mM benzamidine, 1 mM phenylmethylsulfonyl fluoride, 50 mM NaF, 20 mM sodium pyrophosphate, and 1 mM sodium orthovanadate) on ice for 10 min. The cell lysates were collected, sonicated on ice for 3×10 s, and then centrifuged at 15,000*g* for 20 min at 4°C. The resulting supernatants were used as the cell extracts.

MTT Assay

The MTT (3-[4,5-dimethylthiazol-2-yl]-2,5-diphenyltetrazolium bromide) test is a colorimetric assay that measures the percentage of cell survival. MG treated cells were treated with 100 μl of 0.45 g/l MTT solution per dish, incubated at 37°C for 60 min, treated with 100 μl of 20% SDS in DMF:H_2O (1:1), and then incubated overnight at 37°C. Spectrophotometric data were measured using an ELISA reader at a wavelength of 570 nm.

Immunoblots

Immunoblotting was carried out essentially as described in our previous report [Chan, 2005]. Briefly, proteins were resolved by SDS–PAGE, transferred to PVDF membranes, and immunoblotted with anti-JNK, anti-phospho JNK, anti-caspase-3, anti-PARP, anti-PAK (c-19), and anti-PAK2 (N17) antibodies (0.25 μg/ml). The proteins of interest were detected with alkaline phosphatase-conjugated goat anti-rabbit or anti-mouse IgG antibodies and visualized using the CDP-Star™ chemiluminescent substrate, according to the manufacturer's protocol.

Assessment of Necrosis and Apoptosis

Oligonucleosomal DNA fragmentation in apoptotic cells was measured using the Cell Death Detection ELISA^{plus} kit, according to the manufacturer's protocol (Roche Molecular Biochemicals, Mannheim, Germany). Cells (1×10^5) were treated with or without MG at 37°C for the indicated time periods, and spectrophotometric data were obtained with an ELISA reader at 405 nm. Necrosis and apoptosis were further assayed by staining with propidium iodide and Hoechst 33342. Cells were incubated with propidium iodide (1 μg/ml) and Hoechst 33342 (2 μg/ml) at room temperature for 10 min. Under fluorescent microscopy, apoptotic cells were identified as propidium iodide negative cells (having intact plasma membranes that excluded the dye) that showed condensed/fragmented nuclei stained with Hoechst 33342, whereas necrotic cells were identified as being propidium iodide-positive. In each experiment 7–10 independent fields (~600–1,000 nuclei in total) were counted per condition and cell percentages were calculated. Necrosis was also assayed by measurement of the lactate dehydrogenase (LDH) activity present in the culture medium [Behl et al., 1994]. Cells were cultured in 96-well microtiter plates (100 μl medium/well) and the absorption values at 490 nm were determined with an ELISA reader according to the manufacturer's instructions (Promega, Madison, WI). Blanks consisted of samples containing test substances and cell-free medium.

ROS Assay

ROS were measured in arbitrary units using DCF-DA dye. Cells (1.0×10^6) were incubated in 50 μl PBS containing 20 μM DCF-DA for 1 h at 37°C, and relative ROS units were determined using a fluorescence ELISA reader (excitation 485 nm, emission 530 nm). An aliquot of the cell suspension was lysed, the protein concentration was determined, and the results are expressed as arbitrary absorbance units/mg protein.

JNK Assays

JNK activity, as assayed by the presence of phosphorylated c-Jun protein, was analyzed with the AP-1/c-Jun ELISA kit, according to the manufacturer's protocol (Active Motif, Carlsbad, CA). Briefly, AP-1 heterodimeric complexes were collected from cellular nuclear extracts by binding to a consensus 5′-TGA(C/G)TCA-3′ oligonucleotide coated on a 96-well plate. The phospho-c-Jun was assayed using a phospho-c-Jun primary antibody and a secondary horseradish peroxidase-conjugated antibody in a colorimetric reaction.

Cytochrome C Release Assay

Mitochondrial cytochrome C release from MG-treated cells was assayed according to the method described in a previous report [Yang et al., 1997]. Cells (1×10^7) either untreated or MG-treated were harvested by centrifugation at 800*g* at 4°C for 15 min. After washing three times with ice-cold PBS, cell pellets were resuspended in HEPES-buffer (20 mM HEPES, 10 mM KCl, 1.5 mM $MgCl_2$, 1 mM EDTA, 1 mM EGTA, 1 mM DTT, 0.1 mM PMSF, pH 7.5) containing 250 mM sucrose, homogenized, and centrifuged at 800*g* at 4°C for 15 min. Supernatants were centrifuged at 10,000*g* for 15 min at 4°C, and the mitochondrial pellets and supernatants were dissolved in SDS sample buffer, subjected to 15% SDS–PAGE, and analyzed by immunoblotting with a monoclonal antibody against cytochrome C.

Caspase Activity Assays

Caspase-3 activity was measured using the Z-DEVD-AFC fluorogenic substrate, as previously described [Chan et al., 2003; Hsieh et al., 2003]. Caspase-9 activities were assayed using the Colorimetric Caspase-9 Assay Kit (Calbiochem).

Detection of Mitochondrial Membrane Potential (MMP)

Osteoblasts were dispensed to 96-well plates, grown for 24 h, and then incubated with various concentration of MG for 24 h. The fluorescent dyes, DiOC6(3) (20 nM) or TMRE (0.1 μM), were then added to each well, the plate was incubated for 15 min, and fluorescence was measured with a plate spectrofluorometer [excitation: 485 nm (DiOC6(3)) or 535 nm (TMRE); emission: 535 nm (DiOC6(3)) or 590 nm (TMRE)].

Immunoprecipitation and PAK2 Activity Assay

Before immunoprecipitation, cell extracts were diluted to equal protein concentrations (1.0 mg/ml) with cell lysis solution. For immunoprecipitation of the C-terminal catalytic fragment of PAK2, 0.5 ml of cell extract was incubated with 10 μl of anti-PAK2 (C15) antibody (200 μg/ml) at 4°C for 1.5 h, and then further incubated with 40 μl of Protein A-Sepharose CL-4B (30%, v/v) for 1.5 h with shaking. The immunoprecipitates were collected by centrifugation, washed three times with 1 ml of Solution A (20 mM Tris/HCl, pH 7.0, and 0.5 mM DTT) containing 0.5 M NaCl, and resuspended in 40 μl of Solution A. For measurement of PAK2 activity, the immunoprecipitates were incubated in a 50 μl mixture containing 20 mM Tris/HCl, pH 7.0, 0.5 mM DTT, 0.2 mM [γ-p^{32}]ATP, 20 mM $MgCl_2$, and 0.1 mg/ml myelin basic protein (MBP) at room temperature for 10 min with shaking. For determination of ^{32}P incorporation into the MBP protein, 20 μl of each reaction mixture was spotted onto Whatman P81 paper (1×2 cm), which was then washed with 75 mM phosphoric acid and processing as previously described [Reimann et al., 1971].

Inhibition of PAK2 by Anti-Sense Oligonucleotides

PAK2 sense (5′-ATC ATG TCT GAT AAC GGA GAA) and anti-sense (5′-TTC TCC GTT ATC AGA CAT GAT) oligonucleotides, representing amino acids −1 to +7 of human PAK2, were obtained from Life Technologies (Grand Island, NY). The oligonucleotides were synthesized under phosphorothioate-modified conditions, purified by HPLC, and dissolved in 30 mM HEPES buffer, pH 7.0. For transfections, cells grown in 60 mm culture dishes were incubated at 37°C in 1 ml of Opti-MEM I medium (modified

Eagle's minimum essential medium buffered with HEPES and sodium bicarbonate), containing lipofectAMINE4 (12 μg) and oligonucleotides (70 μM) for 72 h (all reagents from Life Technologies). The cells were then subjected to MG treatment, and the cell extracts were analyzed as described above.

Animals, Diets, and Bone Mineral Density Measurement

The effect of MG intake on bone mass was studied in 18 weeks old growing female Wistar rats. The rats were randomly divided into three diet groups of eight rats each. Group one was given a standard diet. Group two was given a standard diet supplemented with 100 μM MG in the drinking water. Group three was given a standard diet supplemented with 200 μM MG in the drinking water. Rats were exposed to MG-containing or control drinking water for 6 months, and the right femur of each rat was analyzed for BMD, using dual energy X-ray absorptiometry (DXA). The in vivo reproducibility was evaluated by measuring the coefficient of variation over five repetitions, with rats repositioned between readings. The same researcher conducted all DXA scans and analyses.

Statistics

Data were analyzed using one-way ANOVA, and differences were evaluated using the Student's *t*-test and analysis of variance. Data are presented as mean ± SD. A P-value <0.05 was defined as indicating a significant difference.

RESULTS

Effects of MG on Human Osteoblasts

Although previous studies have shown that MG treatment causes various cell responses (including apoptosis) in many cell types, no previous work has examined the cytotoxic effects of MG on human osteoblasts, which may be seen as a model for investigating bone density loss in diabetes patients suffering from abnormally high MG levels. To first examine the cytotoxicity of MG on a human osteoblast cell line, we treated cells with various doses of MG at 37°C for 24 h, and measured cell viability and apoptosis. Our results revealed that MG treatment dose-dependently reduced osteoblast cell viability (Fig. 1A). We then investigated whether this MG-induced cell death was due

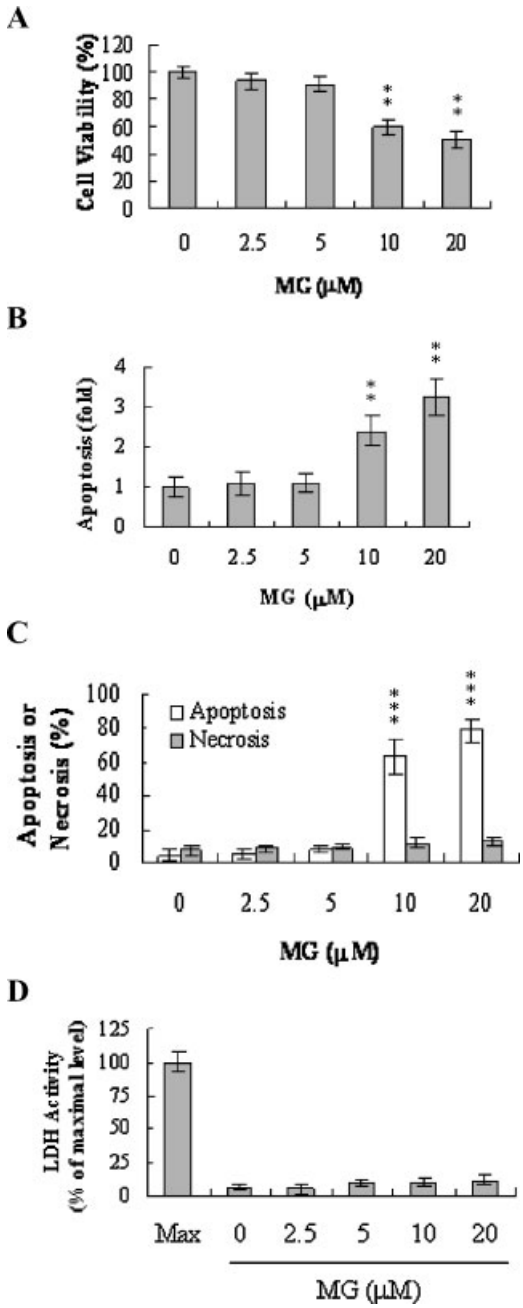

Fig. 1. Effects of MG treatment on human osteoblasts. Osteoblasts were incubated with the indicated concentrations of MG for 24 h. Cell viability was determined using the MTT assay (**A**) and apoptosis was detected by TUNEL assay (**B**). **C**: The percentages of apoptosis and necrosis were determined by propidium iodide and Hoechst 33342 staining. **D**: Necrosis was further assessed by LDH activity released in the culture media of MG-treated osteoblasts. Data are expressed as percent of the maximal level (Max) of LDH activity determined after total cell lysis. Values are presented as mean ± SD of five determinations. $^{**}P < 0.01$ and $^{***}P < 0.001$ versus the untreated control group.

to apoptosis. ELISA-based TUNEL assays revealed that MG treatment caused a significant, dose-dependent increase in DNA fragmentation, which is a hallmark of apoptosis (Fig. 1B). The percentage of apoptotic and necrotic cells was further analyzed by staining with propidium iodide and Hoechst 33342, and necrosis was also assessed by measurement of LDH activity in the culture medium. Our results revealed that the percentage of apoptotic cells increased significantly in cultures exposed to >10 μM MG, whereas the necrotic cell population remained at a relatively low level in these cultures (Fig. 1C,D). These results collectively indicate that MG is cytotoxic to osteoblasts via apoptosis but not necrosis.

ROS Generation and Apoptotic Biochemical Changes in MG-Treated Osteoblasts

As ROS are effective inducers of apoptosis, we used the DCF-DA detection reagent to determine whether ROS are generated in MG-treated osteoblasts. Our results revealed that the intracellular ROS content was significantly increased in human osteoblasts treated with >10 μM MG (Fig. 2A). Activation of the JNK pathway is essential for apoptotic induction in some cell types [Xia et al., 1995; Verheij et al., 1996], and we previously demonstrated that UV irradiation-, MG-, and high glucose-induced apoptosis and caspase-3 activation are mediated by JNK activity [Chan et al., 2003; Chan and Wu, 2004; Hsuuw et al., 2005]. Here, we used immunoblotting and ELISA to examine JNK activity during MG-induced apoptosis. Our results revealed that JNK was dose-dependently activated in MG-treated osteoblasts (Fig. 2B,C). As mitochondrial membrane potential changes and cytochrome C release are directly associated with apoptosis [Li et al., 1997; Zou et al., 1997; Weber et al., 2003], we investigated the effect of MG on mitochondrial membrane potential changes and cytochrome C release in osteoblasts. Our results revealed that osteoblasts treated with 10–20 μM MG showed decreased mitochondrial uptake of DiOC6(3) and TMRE, indicating significant losses of mitochondrial membrane potential (Fig. 2D). Furthermore, immunoblotting of cytosolic fractions from MG-treated and -untreated osteoblasts revealed that cytochrome C was significantly released into the cytosol of MG-treated osteoblasts but not untreated controls (Fig. 2E). As previous studies have shown that the protein expression ratio of Bax versus Bcl-2 is relevant to apoptosis (a high Bax/Bcl-2 ratio is associated with a lower threshold of apoptosis and vice versa), we investigated whether

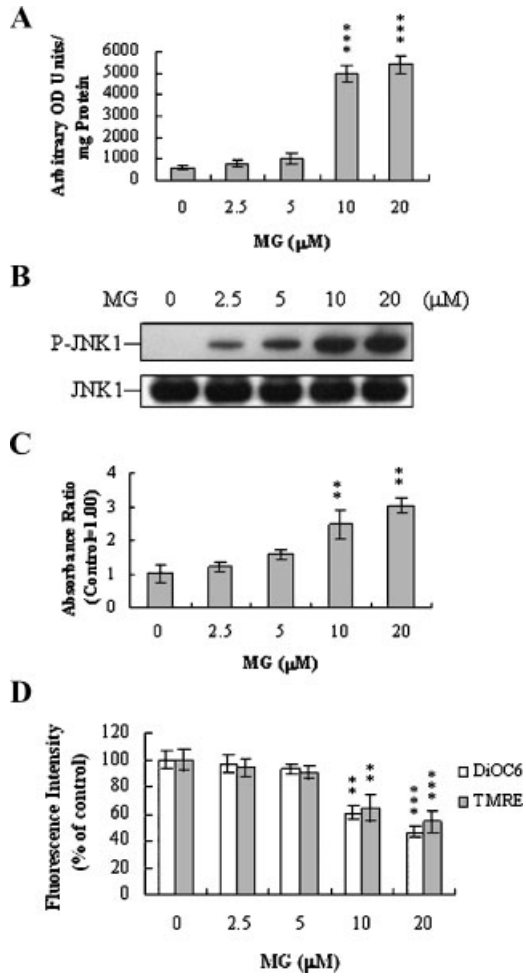

Fig. 2. Apoptotic biochemical changes during MG-induced apoptosis of osteoblasts. **A**: Osteoblasts were preloaded with 10 μM DCF-DA for 1 h, and then treated with or without the indicated concentrations of MG for 1 h. ROS generation was assayed by DCF-DA fluorescence and is expressed as absorbance/mg of protein. **B**: Osteoblasts were incubated with various concentrations of MG for 24 h, and cell extracts (60 μg) were immunoblotted with anti-p-JNK antibody. The **lower panel** shows an immunoblot of JNK1 protein. **C**: JNK/AP-1 activity was evaluated by ELISA detection of phosphorylated c-Jun. The results are expressed with respect to untreated control values, which were arbitrarily set to 1.00. **D**: To examine mitochondrial membrane potential change, cells were then incubated with 40 nM DiOC6(3) or 1 μM TMRE at 37°C for 1 h, and analyzed by spectrofluorometry. **E**: To examine cytochrome C release, cytosolic, and mitochondrial fractions were separated, resolved by 15% SDS–PAGE, and then immunoblotted with an anti-cytochrome C antibody. **F**: Bax and Bcl-2 protein levels were visualized by immunoblotting and analyzed by densitometry. **G**: Values are presented as mean ± SD of five determinations. $^{**}P < 0.01$ and $^{***}P < 0.001$ versus the untreated control group.

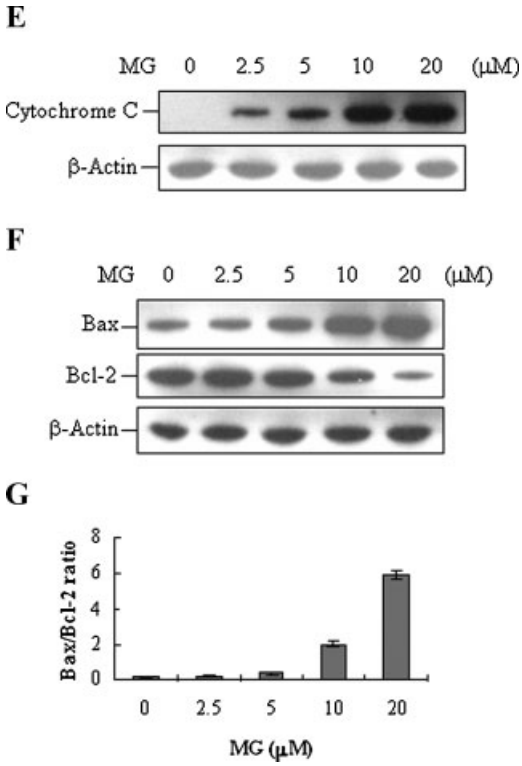

Fig. 2. (*Continued*)

MG-induced apoptosis was associated with changes in the Bax/Bcl-2 ratio in osteoblasts. Immunoblotting revealed that treatment of osteoblasts with 10–20 μM MG was associated with increased Bax protein levels and decreased Bcl-2 protein levels (Fig. 2F). Densitometric analysis quantitatively revealed that MG-treated osteoblasts had a higher Bax/Bcl-2 ratio, which favors apoptosis (Fig. 2G). Collectively, these results indicate that various apoptotic biochemical changes were induced in MG-treated osteoblasts.

Caspase-9, Caspase-3, and PAK2 Activation Are Involved in MG-Induced Apoptosis of Osteoblasts

To further investigate apoptotic signaling during MG-induced apoptosis, we used in vitro ELISA to monitor the activations of caspase-9 and caspase-3, which are known to be involved in apoptosis of multiple cell types triggered by a variety of apoptotic stimuli [Erhardt and Cooper, 1996; Schlegel et al., 1996]. Our results demonstrated that MG treatment of osteoblasts stimulated the activation of caspase-9 (Fig. 3A) and caspase-3 (Fig. 3B,C). Consistent with this finding, cleavage of PARP, the substrate of caspase-3, was triggered by MG treatment of

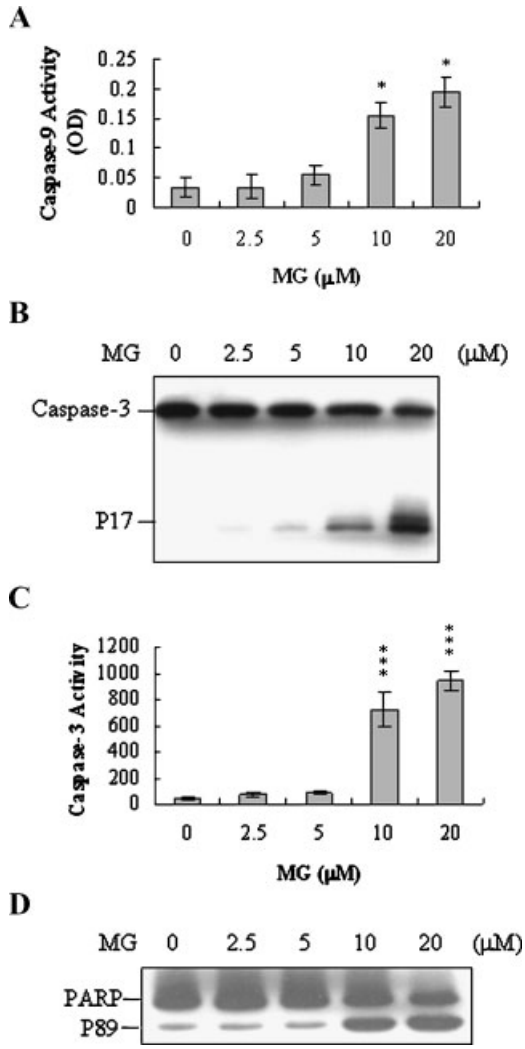

Fig. 3. Activation of caspase-9 and caspase-3 are required for MG-mediated cell death in osteoblasts. Osteoblasts were incubated with various concentrations of MG for 24 h. Caspase-9 activities were assayed using the colorimetric Caspase-9 assay Kit (Calbiochem) (**A**). Cell extracts (60 μg) were immunoblotted with anti-caspase-3 antibodies (**B**). The same cell extracts (60 μg) were analyzed for caspase-3 activity using Z-DEVD-AFC as the substrate (**C**). Cell extracts (40 μg) were immunoblotted using anti-PARP antibody (**D**). P89 (89 kDa) represents the cleavage product of PARP. The data are representative of five independent experiments. Values are presented as mean ± SD of five determinations. $^{*}P < 0.05$ and $^{***}P < 0.001$ versus the value of the untreated control group.

osteoblasts (Fig. 3D). In addition, we also found that caspase-8 activity and Fas protein expression levels did not significantly differ in MG-treated and untreated cells (data not shown). As previous studies have shown that p21-activated kinase (PAK) can be activated during apoptosis and may be involved in apoptotic signaling events [Manser et al., 1994; Martin et al., 1995;

Tang et al., 1998; Chan et al., 1999, 2000], likely via caspase-3 directed proteolysis [Tang et al., 1998; Chan et al., 1999, 2000], we investigated whether cleavage/activation of PAK2 occurred in MG-treated osteoblasts. Immunoblotting and immunoprecipitation kinase activity assays revealed that MG treatment-induced PAK2 cleavage (Fig. 4A) and activation (Fig. 4B), respectively. Collectively, these results indicate that caspase-9 and -3 and PAK2 are involved in MG-induced apoptosis of osteoblasts.

JNK Activation Is Required for Caspase-3 and PAK2 Activation but not ROS Production During MG-Induced Apoptosis

To further determine the relationships among JNK activation, caspase-3 activation, PAK2 activation, and ROS production during MG-induced apoptosis, we examined the effect of the specific JNK inhibitor, SP600125 [Bennett et al., 2001], on MG-treated osteoblasts. SP600125 pretreatment reduced MG-stimulated JNK activity by 50% (Fig. 5A), in association with significant reductions in caspase-3 activation (Fig. 5B), cleavage/activation of PAK2 (Fig. 5C,D), and apoptosis (Fig. 5E), but no such change was observed in ROS production levels (Fig. 5F). These findings indicate that ROS generation is upstream of JNK, which is upstream of caspase-3 activation, PAK2 activation, and subsequent apoptotic biochemical changes during MG-induced apoptosis.

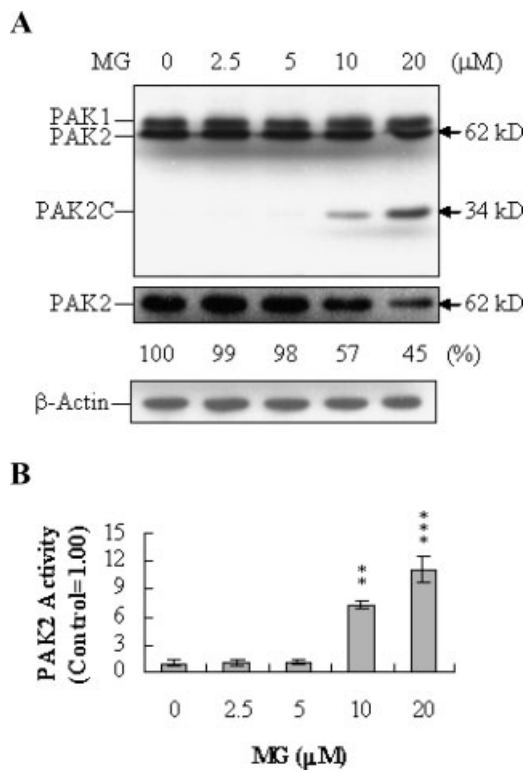

Fig. 4. Activation of PAK2 in MG-treated human osteoblasts. Osteoblasts were incubated with various concentrations of MG for 24 h. **A**: Cell extracts (60 μg) were immunoblotted with anti-αPAK (C19) antibody (**upper panel**) or anti-PAK2 (N17) antibody (**middle panel**). PAK2C represents the C-terminal cleavage product of PAK2. **B**: PAK2 was immunoprecipitated and kinase activities were assayed using myelin basic protein (MBP) as the substrate. Values are presented as mean ± SD of five determinations. $^{**}P < 0.01$ and $^{***}P < 0.001$ versus the untreated control group.

Activation of PAK2 Is Required for MG-Induced Apoptosis in Osteoblasts

To further study the functional role of PAK2 in MG-induced apoptosis, we incubated osteoblasts with anti-sense or sense oligonucleotides against PAK2 for 3 days, subjected the cells to MG treatment, and analyzed cell extracts by immunoblotting with anti-PAK2 (N17) antibodies and immunoprecipitation. Pre-incubation of osteoblasts with the anti-sense oligonucleotide against PAK2 significantly decreased PAK2 protein levels (by ~50%) as compared to untreated controls, whereas the sense oligonucleotide had no such effect (Fig. 6A). Similarly, cells treated with the anti-sense PAK2 oligonucleotide showed activations levels that were approximately 50% those of control cells (Fig. 6B). These decreases in PAK2 protein expression and activation levels were associated with significant decreases in MG-induced apoptosis (Fig. 6C), strongly suggesting that PAK2 expression/activation plays an important role in MG-induced apoptosis of osteoblasts.

MG-Activated IκB Degradation and NF-kB Activation in Osteoblasts

As IκB degradation is a key step in the activation of NF-κB, which can be triggered by MG treatment in hypertensive rat vascular smooth muscle cells [Wu and Juurlink, 2002] and has been associated with MG-induced apoptosis [Kim et al., 2004], we examined the effect of MG on IκB degradation and nuclear translocation of NF-κB in osteoblasts. Treatment of osteoblasts for 24 h with 10–20 μM MG caused marked IκBα degradation and nuclear translocation of NF-κB (Fig. 7), suggesting that MG treatment can induce NF-κB activation in osteoblasts.

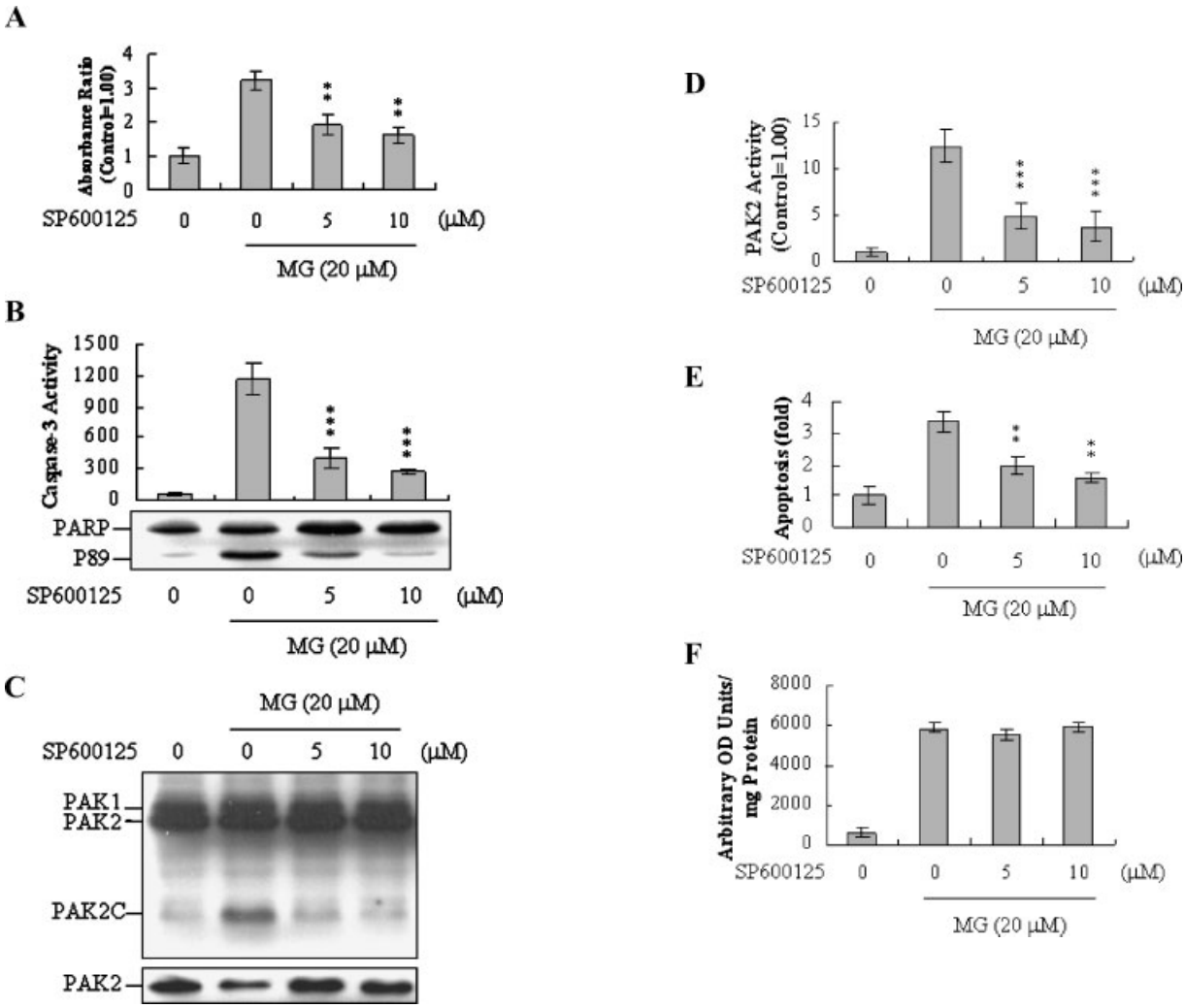

Fig. 5. Effect of a JNK-specific inhibitor (SP600125) on MG-induced JNK activation, caspase-3 activation, and apoptosis of human osteoblasts. Osteoblasts were preincubated with 5 or 10 μM SP600125 at 37°C for 1 h and then incubated with various concentrations of MG with SP600125 for another 24 h. Cell extracts (60 μg) were analyzed for JNK/AP-1 activity (**A**), caspase-3 activity (**B**, **upper panel**), cleavage of PARP (B, **lower panel**), cleavage/activation of PAK2 (**C** and **D**), cell apoptosis (**E**), and generation of ROS (**F**), as described in Figures 2–4. $^{**}P < 0.01$ and $^{***}P < 0.001$ versus the untreated control group.

The Impact of Dietary MG on Bone Mineral Density In Vivo

Lastly, we studied whether the apoptotic effect of MG on osteoblasts might cause bone density injury in vivo. Wistar rats were fed a standard diet supplemented with or without MG (100 or 200 μM) in the drinking water for 6 months. Initial body weights did not differ among the control or MG-treated groups, nor did body weights differ significantly at the end of the 6-month experimental period (data not shown). However, the bone mineral densities (BMD) of whole femurs and distal femurs from rats in the MG-treated groups were significantly lower than those in the control (MG-free) group (Fig. 8). These results suggest that elevated MG levels, such as those found in diabetes patients or induced by continuous long-term consumption of high MG-containing foods, may negatively impact BMD, which is an important indicator for osteoporosis.

DISCUSSION

MG is not only produced through glycolytic metabolism, it is also found as a constituent of various beverages and foodstuffs, including

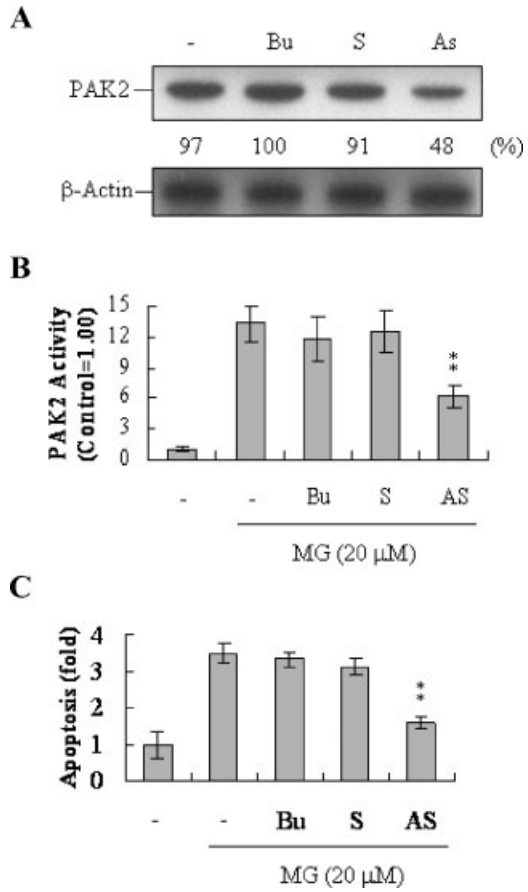

Fig. 6. Effects of anti-sense oligonucleotides against PAK2 on MG-induced apoptosis in osteoblasts. **A**: Osteoblasts were transfected with 70 μM PAK2 sense (S) or anti-sense (AS) oligonucleotides for 72 h. Cell extracts were analyzed by immunoblotting with anti-PAK2 (N17) antibodies. **B**: Cells were transfected with sense (S) or anti-sense (AS) oligonucleotides for 72 h and then subjected to MG (20 μM) treatment for another 24 h. PAK2 was immunoprecipitated and kinase activities were assayed using MBP as the substrate. **C**: Apoptosis was measured by TUNEL method, using the Cell Death Detection ELISA kit. Values are presented as mean ± SD of five determinations. $^{**}P < 0.01$ versus the ''MG-treated only'' group.

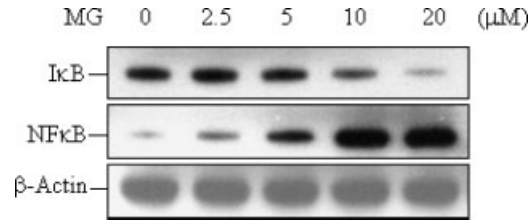

Fig. 7. IκBα degradation and nuclear translocation of NF-κB in MG-treated osteoblasts. Osteoblasts were incubated with various concentrations of MG for 24 h. Cytosolic and nuclear fractions (40 μg each) were separated for immunoblotting analysis using anti-IκBα antibodies (**upper panel**) and anti-NFκB antibodies (**middle panel**), respectively. The **lower panel** shows immunoblot analysis of β-actin from 40 μg total proteins of each cytosolic fraction sample.

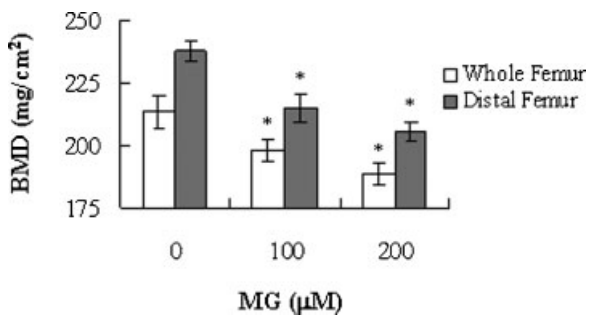

Fig. 8. Effects of MG intake on BMD of rats. DXA was used to assess BMD in whole femurs and distal femurs of rats fed a controlled diet with or without MG (100 or 200 μM) in the drinking water for 6 months. Values are presented as mean ± SD of five determinations. $^{*}P < 0.05$ versus the ''MG-free'' group.

freshly brewed coffee and soy sauce [Kasai et al., 1982]. We herein sought to clarify the possible cytotoxic effects of MG on osteoblasts, a cell type that has not been previously explored in this context. Plasma MG concentrations are typically ~1–2 μM in the general population. In contrast, blood samples from diabetics have been found to contain 3–6 times this level [McLellan et al., 1994], and plasma MG concentrations in diabetics can remain elevated for years. Unlike the relatively narrow range of MG concentrations found in plasma, however, tissue levels of MG may vary widely. For example, as much as 310 μM MG can be found in Chinese hamster ovary (CHO) cells [Chaplen et al., 1998]. Thus, we feel confident that although our utilized MG concentrations exceeded those observed in the blood of human diabetes mellitus (DM) patients (we used 10–20 μM in the cellular model and 100–200 μM in the animal model vs. 3–10 μM in human DM plasma), our findings remain relevant to the study of apoptotic signaling during MG-induced cell injury in human osteoblasts.

Our results revealed that MG has cytotoxic effects on human osteoblasts in vitro and in vivo. This cytotoxicity occurred via apoptosis, not necrosis (Fig. 1), and involved the activation of mitochondrial processes and caspases (Figs. 2–4), a signal transduction pathway often associated with oxidative stress-mediated cell injury. Consistent with this observation, our experiments also demonstrated that intracellular ROS were generated in MG-treated osteoblasts (Fig. 2A). MG treatment could

potentially increase intracellular ROS levels via glycation reactions, depletion of cellular GSH, and/or inactivation of ROS scavenger enzymes [Yim et al., 1995; Lee et al., 1998; Oya et al., 1999]. We previously demonstrated that ROS generation is an upstream regulator of apoptotic signaling during apoptosis induced by various environmental stress stimuli [Chan et al., 2003; Chan and Wu, 2004; Chan, 2005]. In addition, antioxidant-mediated inhibition of ROS generation during apoptosis has been found to prevent JNK activation and subsequent apoptotic biochemical changes [Chan et al., 2003; Chan and Wu, 2004; Chan, 2005]. Consistent with these previous findings, our results revealed that ROS generation is critically involved in MG-induced apoptosis.

JNK plays roles in many cellular events, including entry into apoptosis [Xia et al., 1995; Verheij et al., 1996; Seimiya et al., 1997]. Recently, apoptosis signal-regulating kinase 1 (ASK1), a mitogen-activated protein kinase/extracellular signal-regulated kinase kinase (MEKK) family member, was reported to be activated by various agents, including MG [Gotoh and Cooper, 1998; Saitoh et al., 1998; Chen et al., 1999; Hsuuw et al., 2005]. Expression of a dominant negative inactive mutant form of ASK1 inhibited MG-induced apoptosis in Jurkat cells and reduced JNK phosphorylation, which is necessary for MG-induced apoptotic signal transduction [Du et al., 2000]. These observations indicate that ASK1 and JNK play critical roles in MG-induced apoptosis. Here, we demonstrated that MG treatment of osteoblasts stimulated ROS formation (Fig. 2A), JNK activation (Fig. 2B), and subsequent apoptotic biochemical changes (Figs. 2 and 3). Moreover, using a specific JNK inhibitor, SP600125, we demonstrated that MG-induced caspase-3 activation and apoptosis in osteoblasts are mediated by JNK activity (Fig. 5). Taken together, these observations support the hypothesis that ROS generation and ROS-mediated JNK activation, which are important triggers for Bax/Bcl-2 ratio decreases, cytochrome C release, and caspase activation, are critically involved in MG-induced apoptosis of osteoblasts.

Our group and other researchers have shown that PAK2 is a targeting substrate for caspases activated by various apoptotic stimuli [Lee et al., 1997; Rudel and Bokoch, 1997; Chan et al., 1998, 1999; Tang et al., 1998]. However, the functional role of the caspase-generated C-terminal active fragment of PAK2 remains obscure. In this report, we used anti-sense techniques to provide direct evidence that PAK2 activation plays a critical role in MG-induced apoptosis (Fig. 6A–C). This finding may explain the previous observation that apoptosis was delayed by transfection of dominant-negative PAK2 (either full-length or an N-terminally truncated form) into CHO cells stably expressing a CD4-Fas chimera [Lee et al., 1997]. A recent study further showed that an anti-activated PAK2 polyclonal antibody recognized many phosphoproteins in mitotic HeLa and A431 cells, including lamins A and C [Tsai et al., 2005]. These results show that the PAKs are heavily involved in cell-cycle control. Here, we additionally show the involvement of PAK2 in MG-directed apoptosis of osteoblasts. Future work will be required to identify the apoptosis-related target substrates of active PAK2.

In terms of a possible mechanism for the involvement of PAK2 in MG-induced apoptosis, two previous studies showed that transfection of constitutively activated forms of Rac and Cdc42 into cultured cells led to potent activation of JNK [Coso et al., 1995]. These findings suggest that PAK may be placed in the Rac/Cdc42-mediated JNK activation pathway, possibly as an upstream regulator of JNK. This notion was strongly supported in a recent report that transfection of N-terminal truncated PAK2 and constitutively active PAK1 into cultured cells led to JNK activation [Lee et al., 1997]. In contrast, we herein showed that JNK functions upstream of PAK2 activation during MG-induced apoptosis (Fig. 3), suggesting that these molecules may act either upstream or downstream of each other in cell signaling pathway. Future work will be required to address the relationship(s) between PAK2 and JNK during apoptosis.

ROS are known to regulate activation of NF-κB [Siebenlist et al., 1994], a p50/p65 heterodimer that is localized in the cytosol of resting cells, held there by interactions with IκB inhibitory proteins [Baeuerle and Henkel, 1994]. Following stimulation, IκB may be phosphorylated, ubiquitinated, and degraded, allowing NF-κB to translocate into the nucleus. Several recent studies have reported that NF-κB activation by oxidative stress is involved in apoptotic cell death [Romeo et al., 2002; Kim

et al., 2004], and a putative inhibitor of NF-κB was shown to block MG-induced apoptosis in bovine retinal pericytes [Kim et al., 2004]. Interestingly, PAK1 was found to act as an upstream regulator in Helicobacter pylori-induced activation of NF-κB in epithelial cells, but was not involved in NF-κB activation by TNFα or phorbol 12-myristate 13-acetate, indicating that different NF-κB-activating stimuli may use alternate signaling components [Foryst-Ludwig and Naumann, 2000]. We herein showed that MG could induce IκB degradation and nuclear translocation of NF-κB (Fig. 7). Future work will be required to determine whether PAK2 activation, which we also found to be involved in MG-induced apoptosis in osteoblasts (Fig. 6), is associated with NF-κB in this context.

Lastly, given the ability of MG to induce apoptosis or cell injury in osteoblasts in vitro, we examined the effects of MG on bone density in an animal assay model. Our results revealed that rats given 100 or 200 μM MG in their drinking water for 6 months showed significant decreases in BMD versus untreated control rats (Fig. 8), suggesting that short-term acute exposure to MG may negatively affect bone density. Future work will be required to examine the longer-term effects of lower doses (~5–10 μM) of MG, and whether these findings correlate with the bone loss observed in DM patients having elevated plasma MG levels.

In conclusion, we herein show that MG treatment induces apoptosis in osteoblasts, in association with various apoptotic biochemical changes, including ROS generation, JNK activation, decreased Bax/Bcl-2 ratios, mitochondrial membrane potential changes, cytochrome C release, and activation of caspase-9, caspase-3, and PAK2. Our results revealed that JNK activation is required for the mitochondrial apoptotic signaling processes, and that PAK2 activation is critical for MG-induced apoptosis in osteoblasts. These results coupled with our previous studies support the hypothesis that MG-triggered apoptotic signaling in osteoblasts occurs as follows: MG treatment→ ROS generation→JNK activation→increased Bax/Bcl-2 ratio→mitochondrial membrane potential changes→cytochrome C release→ caspase-3 activation→PAK2 cleavage/activation→apoptosis. Lastly, we showed that MG treatment not only triggers apoptosis in an osteoblast cell culture model, but also decreases BMD in an animal model. These findings provide the first preliminary evidence that the increased MG levels found in DM patients or in individuals with high dietary MG intake may be a risk factor for human osteoporosis.

REFERENCES

Anderson P. 1997. Kinase cascades regulating entry into apoptosis. Microbiol Mol Biol Rev 61:33–46.

Baeuerle PA, Henkel T. 1994. Function and activation of NF-kappa B in the immune system. Annu Rev Immunol 12:141–179.

Behl C, Davis JB, Lesley R, Schubert D. 1994. Hydrogen peroxide mediates amyloid beta protein toxicity. Cell 77: 817–827.

Bennett BL, Sasaki DT, Murray BW, O'Leary EC, Sakata ST, Xu W, Leisten JC, Motiwala A, Pierce S, Satoh Y, Bhagwat SS, Manning AM, Anderson DW. 2001. SP600125, an anthrapyrazolone inhibitor of Jun N-terminal kinase. Proc Natl Acad Sci USA 98:13681–13686.

Bouillon R. 1991. Diabetic bone disease. Calcif Tissue Int 49:155–160.

Bourajjaj M, Stehouwer CD, van Hinsbergh VW, Schalkwijk CG. 2003. Role of methylglyoxal adducts in the development of vascular complications in diabetes mellitus. Biochem Soc Trans 31:1400–1402.

Brownlee M, Cerami A, Vlassara H. 1988. Advanced glycosylation end products in tissue and the biochemical basis of diabetic complications. N Engl J Med 318:1315–1321.

Buttke TM, Sandstrom PA. 1994. Oxidative stress as a mediator of apoptosis. Immunol Today 15:7–10.

Chan WH. 2005. Effect of resveratrol on high glucose-induced stress in human leukemia K562 cells. J Cell Biochem 94:1267–1279.

Chan WH, Wu HJ. 2004. Anti-apoptotic effects of curcumin on photosensitized human epidermal carcinoma A431 cells. J Cell Biochem 92:200–212.

Chan WH, Yu JS, Yang SD. 1998. Heat shock stress induces cleavage and activation of PAK2 in apoptotic cells. J Protein Chem 17:485–494.

Chan WH, Yu JS, Yang SD. 1999. PAK2 is cleaved and activated during hyperosmotic shock-induced apoptosis via a caspase-dependent mechanism: Evidence for the involvement of oxidative stress. J Cell Physiol 178:397–408.

Chan WH, Yu JS, Yang SD. 2000. Apoptotic signalling cascade in photosensitized human epidermal carcinoma A431 cells: Involvement of singlet oxygen, c-Jun N-terminal kinase, caspase-3 and p21-activated kinase 2. Biochem J 351:221–232.

Chan WH, Wu CC, Yu JS. 2003. Curcumin inhibits UV irradiation-induced oxidative stress and apoptotic biochemical changes in human epidermoid carcinoma A431 cells. J Cell Biochem 90:327–338.

Chaplen FW, Fahl WE, Cameron DC. 1998. Evidence of high levels of methylglyoxal in cultured Chinese hamster ovary cells. Proc Natl Acad Sci USA 95:5533–5538.

Chen Z, Seimiya H, Naito M, Mashima T, Kizaki A, Dan S, Imaizumi M, Ichijo H, Miyazono K, Tsuruo T. 1999.

ASK1 mediates apoptotic cell death induced by genotoxic stress. Oncogene 18:173–180.
Coso OA, Chiariello M, Yu JC, Teramoto H, Crespo P, Xu N, Miki T, Gutkind JS. 1995. The small GTP-binding proteins Rac1 and Cdc42 regulate the activity of the JNK/SAPK signaling pathway. Cell 81:1137–1146.
Du J, Suzuki H, Nagase F, Akhand AA, Yokoyama T, Miyata T, Kurokawa K, Nakashima I. 2000. Methylglyoxal induces apoptosis in Jurkat leukemia T cells by activating c-Jun N-terminal kinase. J Cell Biochem 77: 333–344.
Erhardt P, Cooper GM. 1996. Activation of the CPP32 apoptotic protease by distinct signaling pathways with differential sensitivity to Bcl-xL. J Biol Chem 271:17601–17604.
Foryst-Ludwig A, Naumann M. 2000. p21-activated kinase 1 activates the nuclear factor kappa B (NF-kappa B)-inducing kinase-Ikappa B kinases NF-kappa B pathway and proinflammatory cytokines in Helicobacter pylori infection. J Biol Chem 275:39779–39785.
Frost JA, Xu S, Hutchison MR, Marcus S, Cobb MH. 1996. Actions of Rho family small G proteins and p21-activated protein kinases on mitogen-activated protein kinase family members. Mol Cell Biol 16:3707–3713.
Gerozissis K. 2003. Brain insulin: Regulation, mechanisms of action and functions. Cell Mol Neurobiol 23:1–25.
Gotoh Y, Cooper JA. 1998. Reactive oxygen species- and dimerization-induced activation of apoptosis signal-regulating kinase 1 in tumor necrosis factor-alpha signal transduction. J Biol Chem 273:17477–17482.
Hsieh YJ, Wu CC, Chang CJ, Yu JS. 2003. Subcellular localization of Photofrin determines the death phenotype of human epidermoid carcinoma A431 cells triggered by photodynamic therapy: When plasma membranes are the main targets. J Cell Physiol 194:363–375.
Hsuuw YD, Chang CK, Chan WH, Yu JS. 2005. Curcumin prevents methylglyoxal-induced oxidative stress and apoptosis in mouse embryonic stem cells and blastocysts. J Cell Physiol 205:379–386.
Jakobi R, Chen CJ, Tuazon PT, Traugh JA. 1996. Molecular cloning and sequencing of the cytostatic G protein-activated protein kinase PAK I. J Biol Chem 271:6206–6211.
Kang Y, Edwards LG, Thornalley PJ. 1996. Effect of methylglyoxal on human leukaemia 60 cell growth: Modification of DNA G1 growth arrest and induction of apoptosis. Leuk Res 20:397–405.
Kasai H, Kumeno K, Yamaizumi Z, Nishimura S, Nagao M, Fujita Y, Sugimura T, Nukaya H, Kosuge T. 1982. Mutagenicity of methylglyoxal in coffee. Gann 73:681–683.
Kayath MJ, Tavares EF, Dib SA, Vieira JG. 1998. Prospective bone mineral density evaluation in patients with insulin-dependent diabetes mellitus. J Diabet Complications 12:133–139.
Kim J, Son JW, Lee JA, Oh YS, Shinn SH. 2004. Methylglyoxal induces apoptosis mediated by reactive oxygen species in bovine retinal pericytes. J Korean Med Sci 19:95–100.
Lee N, MacDonald H, Reinhard C, Halenbeck R, Roulston A, Shi T, Williams LT. 1997. Activation of hPAK65 by caspase cleavage induces some of the morphological and biochemical changes of apoptosis. Proc Natl Acad Sci USA 94:13642–13647.
Lee C, Yim MB, Chock PB, Yim HS, Kang SO. 1998. Oxidation-reduction properties of methylglyoxal-modified protein in relation to free radical generation. J Biol Chem 273:25272–25278.
Li P, Nijhawan D, Budihardjo I, Srinivasula SM, Ahmad M, Alnemri ES, Wang X. 1997. Cytochrome c and dATP-dependent formation of Apaf-1/caspase-9 complex initiates an apoptotic protease cascade. Cell 91:479–489.
Manser E, Leung T, Salihuddin H, Zhao ZS, Lim L. 1994. A brain serine/threonine protein kinase activated by Cdc42 and Rac1. Nature 367:40–46.
Martin GA, Bollag G, McCormick F, Abo A. 1995. A novel serine kinase activated by rac1/CDC42Hs-dependent autophosphorylation is related to PAK65 and STE20. EMBO J 14:1970–1978.
Martins LM, Kottke T, Mesner PW, Basi GS, Sinha S, Frigon N, Jr., Tatar E, Tung JS, Bryant K, Takahashi A, Svingen PA, Madden BJ, McCormick DJ, Earnshaw WC, Kaufmann SH. 1997. Activation of multiple interleukin-1beta converting enzyme homologues in cytosol and nuclei of HL-60 cells during etoposide-induced apoptosis. J Biol Chem 272:7421–7430.
McLellan AC, Thornalley PJ, Benn J, Sonksen PH. 1994. Glyoxalase system in clinical diabetes mellitus and correlation with diabetic complications. Clin Sci (Lond) 87:21–29.
Messier C, Gagnon M. 1996. Glucose regulation and cognitive functions: Relation to Alzheimer's disease and diabetes. Behav Brain Res 75:1–11.
Nicholson DW, Thornberry NA. 1997. Caspases: Killer proteases. Trends Biochem Sci 22:299–306.
Nicodemus KK, Folsom AR. 2001. Type 1 and type 2 diabetes and incident hip fractures in postmenopausal women. Diabetes Care 24:1192–1197.
Okado A, Kawasaki Y, Hasuike Y, Takahashi M, Teshima T, Fujii J, Taniguchi N. 1996. Induction of apoptotic cell death by methylglyoxal and 3-deoxyglucosone in macrophage-derived cell lines. Biochem Biophys Res Commun 225:219–224.
Oya T, Hattori N, Mizuno Y, Miyata S, Maeda S, Osawa T, Uchida K. 1999. Methylglyoxal modification of protein. Chemical and immunochemical characterization of methylglyoxal-arginine adducts. J Biol Chem 274: 18492–18502.
Reichlin M. 1980. Use of glutaraldehyde as a coupling agent for proteins and peptides. Methods Enzymol 70:159–165.
Reimann EM, Walsh DA, Krebs EG. 1971. Purification and properties of rabbit skeletal muscle adenosine 3′,5′-monophosphate-dependent protein kinases. J Biol Chem 246:1986–1995.
Romeo G, Liu WH, Asnaghi V, Kern TS, Lorenzi M. 2002. Activation of nuclear factor-kappaB induced by diabetes and high glucose regulates a proapoptotic program in retinal pericytes. Diabetes 51:2241–2248.
Rudel T, Bokoch GM. 1997. Membrane and morphological changes in apoptotic cells regulated by caspase-mediated activation of PAK2. Science 276:1571–1574.
Saitoh M, Nishitoh H, Fujii M, Takeda K, Tobiume K, Sawada Y, Kawabata M, Miyazono K, Ichijo H. 1998. Mammalian thioredoxin is a direct inhibitor of apoptosis signal-regulating kinase (ASK) 1. EMBO J 17:2596–2606.
Schlegel J, Peters I, Orrenius S, Miller DK, Thornberry NA, Yamin TT, Nicholson DW. 1996. CPP32/apopain is a key

interleukin 1 beta converting enzyme-like protease involved in Fas-mediated apoptosis. J Biol Chem 271: 1841–1844.

Seimiya H, Mashima T, Toho M, Tsuruo T. 1997. c-Jun NH2-terminal kinase-mediated activation of interleukin-1beta converting enzyme/CED-3-like protease during anticancer drug-induced apoptosis. J Biol Chem 272: 4631–4636.

Shipanova IN, Glomb MA, Nagaraj RH. 1997. Protein modification by methylglyoxal: Chemical nature and synthetic mechanism of a major fluorescent adduct. Arch Biochem Biophys 344:29–36.

Siebenlist U, Franzoso G, Brown K. 1994. Structure, regulation and function of NF-kappa B. Annu Rev Cell Biol 10:405–455.

Tang TK, Chang WC, Chan WH, Yang SD, Ni MH, Yu JS. 1998. Proteolytic cleavage and activation of PAK2 during UV irradiation-induced apoptosis in A431 cells. J Cell Biochem 70:442–454.

Tsai IC, Hsieh YJ, Lyu PC, Yu JS. 2005. Anti-phosphopeptide antibody, P-STM as a novel tool for detecting mitotic phosphoproteins: Identification of lamins A and C as two major targets. J Cell Biochem 94:967–981.

Tsujimoto Y, Shimizu S. 2000. Bcl-2 family: Life-or-death switch. FEBS Lett 466:6–10.

Uchida K, Khor OT, Oya T, Osawa T, Yasuda Y, Miyata T. 1997. Protein modification by a Maillard reaction intermediate methylglyoxal. Immunochemical detection of fluorescent 5-methylimidazolone derivatives in vivo. FEBS Lett 410:313–318.

Verheij M, Bose R, Lin XH, Yao B, Jarvis WD, Grant S, Birrer MJ, Szabo E, Zon LI, Kyriakis JM, Haimovitz-Friedman A, Fuks Z, Kolesnick RN. 1996. Requirement for ceramide-initiated SAPK/JNK signalling in stress-induced apoptosis. Nature 380:75–79.

Weber T, Dalen H, Andera L, Negre-Salvayre A, Auge N, Sticha M, Lloret A, Terman A, Witting PK, Higuchi M, Plasilova M, Zivny J, Gellert N, Weber C, Neuzil J. 2003. Mitochondria play a central role in apoptosis induced by alpha-tocopheryl succinate, an agent with antineoplastic activity: Comparison with receptor-mediated pro-apoptotic signaling. Biochemistry 42:4277–4291.

Wu L, Juurlink BH. 2002. Increased methylglyoxal and oxidative stress in hypertensive rat vascular smooth muscle cells. Hypertension 39:809–814.

Xia Z, Dickens M, Raingeaud J, Davis RJ, Greenberg ME. 1995. Opposing effects of ERK and JNK-p38 MAP kinases on apoptosis. Science 270:1326–1331.

Yamagishi S, Nakamura K, Inoue H. 2005. Possible participation of advanced glycation end products in the pathogenesis of osteoporosis in diabetic patients. Med Hypotheses 65:1013–1015.

Yang J, Liu X, Bhalla K, Kim CN, Ibrado AM, Cai J, Peng TI, Jones DP, Wang X. 1997. Prevention of apoptosis by Bcl-2: Release of cytochrome c from mitochondria blocked. Science 275:1129–1132.

Yim HS, Kang SO, Hah YC, Chock PB, Yim MB. 1995. Free radicals generated during the glycation reaction of amino acids by methylglyoxal. A model study of protein-cross-linked free radicals. J Biol Chem 270:28228–28233.

Yu JS, Yang SD. 1994. Okadaic acid, a serine/threonine phosphatase inhibitor, induces tyrosine dephosphorylation/inactivation of protein kinase FA/GSK-3 alpha in A431 cells. J Biol Chem 269:14341–14344.

Zhang S, Han J, Sells MA, Chernoff J, Knaus UG, Ulevitch RJ, Bokoch GM. 1995. Rho family GTPases regulate p38 mitogen-activated protein kinase through the downstream mediator Pak1. J Biol Chem 270:23934–23936.

Zou H, Henzel WJ, Liu X, Lutschg A, Wang X. 1997. Apaf-1, a human protein homologous to C. elegans CED-4, participates in cytochrome c-dependent activation of caspase-3. Cell 90:405–413.